

07.2;07.3;08.3

Half-disk microlasers with half-ring contact based on InGaAs/GaAs quantum well-dots with high output power

© F.I. Zubov¹, Yu.M. Shernyakov², A.A. Beckman², E.I. Moiseev¹, Yu.A. Salii (Guseva)^{2,1}, M.M. Kulagina², N.A. Kalyuzhnyy², S.A. Mintairov², M.V. Maximov¹

¹ Alferov University Petersburg, Russia

² Ioffe Institute, St. Petersburg, Russia

E-mail: fedyazu@mail.ru

Received November 29, 2023

Revised December 6, 2023

Accepted December 6, 2023

Light-current characteristics of half-disk microlasers with active region based on InGaAs/GaAs quantum well-dots emitting at wavelength of 1090 nm are studied. The devices were fabricated by cleaving 200 μm in diameter microdisks with 10 μm wide ring contacts. The maximal achieved CW output optical power amounted to 110 mW. Lasing was observed up to 113°C.

Keywords: microlaser, half-disk resonator, whispering gallery modes, quantum well-dots.

DOI: 10.21883/0000000000

Compact coherent radiation sources (microlasers) are currently attracting considerable attention due to the potential of their application in data transmission over short distances, diagnostics (including lab-on-a-chip devices), sensorics, and other rapidly developing fields of modern science and technology. In certain applications (e.g., photonic integrated circuits), output radiation needs to propagate laterally, parallel to the substrate surface. This type of radiation outcoupling is implemented in microdisk lasers [1], which also have several other advantages, such as the simplicity of epitaxial synthesis and subsequent post-growth processing, low threshold currents, and high operating temperatures. The emission of output power into an azimuthal angle of 360° can be regarded as a disadvantage of microdisk lasers. It has been proposed in [2] that directed light outcoupling may be achieved in half-disk lasers produced by cleaving disk lasers along their diameter. It was demonstrated theoretically that these lasers support whispering-gallery modes and the feedback in such cavities is maintained by reflection from the cleaved facet, which also serves for radiation outcoupling. A half-disk laser 285 μm in diameter with an active region based on two GaInSbAs/GaAlSb(As) quantum wells demonstrated lasing at a wavelength of 2.13 μm , and the output power was around 15 mW. A similar approach was utilized in [3]: directed radiation outcoupling was implemented by cleaving a small (2 μm in width) segment of an AlGaInAs/InP microdisk laser 16 μm in diameter. However, this device operated only at temperatures no higher than 10°C, and the output power was fairly low (13 μW).

We have already examined half-disk and half-ring lasers with an active region based on InGaAs/GaAs quantum well-dots (QWDs) in [4–6]. It was found that they have several advantages over common disk and ring lasers of the same diameter: directed radiation outcoupling and higher

output power and efficiency. A continuous-wave output power of approximately 70 mW was achieved in half-disk lasers 200 μm in diameter [5]. The maximum continuous-wave power of half-disk lasers 100 μm in diameter with *p*-side down bonding was 30 mW, and lasing was observed up to a temperature of 93°C [6]. Quasi-single-frequency lasing with a high side-mode suppression ratio (more than 20 dB) was demonstrated [5]. The maximum frequency of small-signal modulation of a half-disk laser 100 μm in diameter at the –3 dB level was 4.6 GHz [6].

In the present study, half-disk lasers 200 μm in diameter with an active region based on InGaAs/GaAs QWDs are examined. An increase in the number of QWD layers in the active region (from five to seven) and a reduction in the metallic contact width (from 15 to 10 μm) helped raise considerably the output optical power and the maximum operating temperature of devices relative to the levels reported earlier.

The laser heterostructure was grown by metalorganic vapor phase epitaxy on an n^+ -GaAs substrate misoriented by 6° with respect to plane (100) and included the following sequence of layers (starting from the n^+ -substrate): an Al_{0.4}Ga_{0.6}As layer 1 μm in thickness doped with silicon to $2 \cdot 10^{18} \text{ cm}^{-2}$; an Al_{0.4}Ga_{0.6}As layer 0.5 μm in thickness doped with silicon to $7 \cdot 10^{17} \text{ cm}^{-2}$; a GaAs waveguide with an approximate thickness of 0.72 μm and the active region at its center; an Al_{0.4}Ga_{0.6}As layer 0.5 μm in thickness doped with zinc to $7 \cdot 10^{17} \text{ cm}^{-2}$; an Al_{0.4}Ga_{0.6}As layer 0.7 μm in thickness doped with zinc to $2 \cdot 10^{18} \text{ cm}^{-2}$; and a contact GaAs layer 0.15 μm in thickness doped with zinc to $1 \cdot 10^{19} \text{ cm}^{-2}$. The Al_{0.4}Ga_{0.6}As emitter composition was chosen so as to provide both strong optical confinement of the optical mode and the needed doping levels. The active region contained seven layers of In_{0.4}Ga_{0.6}As/GaAs QWDs the properties of which have been discussed in detail in [7].

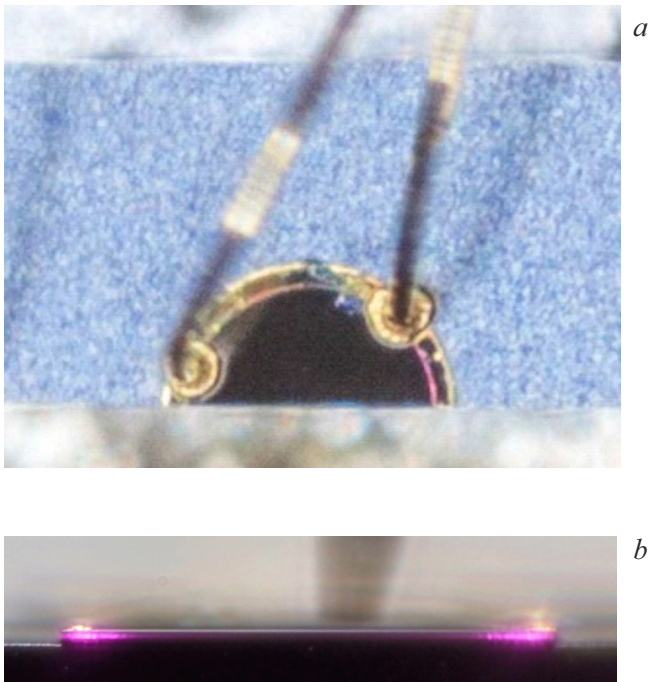


Figure 1. Optical micrographs. *a* — Top view of a half-disk microlaser ($\varnothing 200\ \mu\text{m}$) with golden microwires bonded to it; *b* — view of the cleaved edge of the device under pumping above the lasing threshold.

QWD layers were separated by GaAs spacers 40 nm in thickness. Each QWD layer was formed by depositing eight $\text{In}_{0.4}\text{Ga}_{0.6}\text{As}$ monolayers. This resulted in the fabrication of an ultradense array of In-enriched islands in a residual In-depleted quantum well.

Microdisk cavities with a diameter of $200\ \mu\text{m}$ were fabricated first with the use of photolithography and plasma chemical etching. Etching was performed to a depth of $6.5\ \mu\text{m}$ through the active region and the lower emitter. The side surfaces of cavities were not passivated. Ring metallic AgMn/Ni/Au contacts were formed on the surface of p^+ -GaAs contact layers of the microdisks. The width of the rings was $10\ \mu\text{m}$. The outer diameter of ring contacts was made several micrometers smaller than the diameter of the microdisk cavity in order to exclude current injection into regions located in the immediate vicinity of its side surface. This provided the suppression of parasitic surface recombination on the side walls. The GaAs substrate was then thinned down approximately to $160\ \mu\text{m}$, and a solid metallic contact was formed on its back side. Structures containing one or several half-disk microlasers were produced after that by cleaving chips with a few microdisks (Fig. 1, *a*). Precision cleaving was carried out using a Finetech Fineplacer Lambda 2 die bonder with accurate positioning of the cleaving tool, which made it possible to limit the deviation of cleavage lines from the axis of half-disks to $2\ \mu\text{m}$. Chips with microlasers were soldered to copper heatsinks with their p -contacts facing up. Pumping of half-disks was performed either with the

use of gold wires ($\varnothing 18\ \mu\text{m}$) bonded to half-ring contacts by thermosonic bonding (Fig. 1, *a*) or via a tungsten probe (Fig. 1, *b*). The series resistance of the device was $4.0\ \Omega$.

Current–voltage and light–current characteristics (CVCs and LCCs) were measured in the continuous-wave mode. A calibrated Ge photodiode $1 \times 1\ \text{cm}$ in size positioned in the immediate vicinity of a microlaser (the radiation collection angle was 136°) was used to determine the absolute value of output power. Emission spectra were recorded with a Yokogawa AQ6370C optical spectrum analyzer. The threshold current was determined by finding the point of intersection between the abscissa axis and a linear extrapolation of the LCC section under pumping slightly above the threshold kink (Fig. 2). Measurements were performed at temperatures ranging from 20 to 115°C . The temperature of microlasers was stabilized with a Peltier element.

As was demonstrated in our earlier studies [4,6] and the work of another research group [2], nodes of the most intensive high-Q optical modes of half-disk cavities, which are involved in lasing, are positioned close to the periphery of a cavity. These are the regions of a half-disk laser that emit intense radiation (Fig. 1, *b*) due to non-total reflection from the cleaved facet (the reflection coefficient was approximately 0.3). The use of a half-ring contact allows one to confine injection to the regions located near the edge of a half-disk laser and suppress pumping of the central part, where the intensity of optical modes is low. This provides an opportunity to reduce the threshold current and raise the efficiency of a half-disk laser with a half-ring contact relative to the corresponding parameters of a half-disk laser with a solid contact [6].

Figure 2 shows the CVC and LCC of a half-disk laser measured under continuous-wave pumping at a heatsink temperature of 20°C . The output power reaches its maximum of 110 mW at a current of 0.4 A and starts decreasing at higher currents due to overheating of the active region. The LCC has a kink at an injection current of 0.2 A, which is apparently attributable to an abrupt change in the mode composition of emission. Lasing is quenched completely at currents above 0.53 A. A low optical power observed above the lasing quenching current is attributable to spontaneous emission. The presented LCCs were successfully reproduced numerous times with the current increasing and decreasing in cycles, indicating that overheating does not induce degradation of the laser. The maximum wall-plug efficiency of a half-disk laser was slightly above 18% (Fig. 2).

The lasing wavelength was around 1090 nm (see the inset in Fig. 2). The emission spectrum is a multimode one, and modes are spaced 0.5 nm apart. This corresponds roughly to the distance between resonance wavelengths of whispering-gallery modes of the same radial order (free spectral range) of a microdisk cavity $200\ \mu\text{m}$ in diameter. As the injection current rises, the number of modes in the emission spectrum increases, and the spectral distance between the outermost modes extends to 5 nm. The approximate half-power

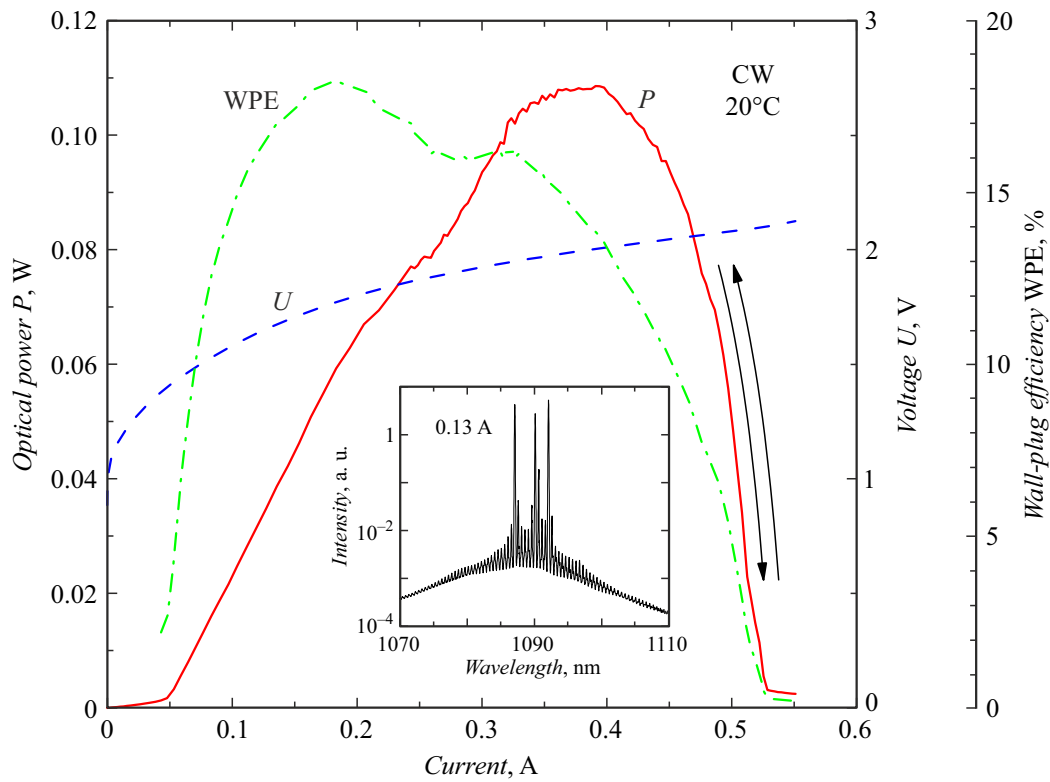


Figure 2. Light–current (solid curve) and current–voltage (dashed curve) characteristics and wall-plug efficiency (WPE) (dash-and-dot curve) of a half-disk laser measured under continuous-wave pumping at a heatsink temperature of 20°C. This insert shows the lasing spectrum at 0.13 A.

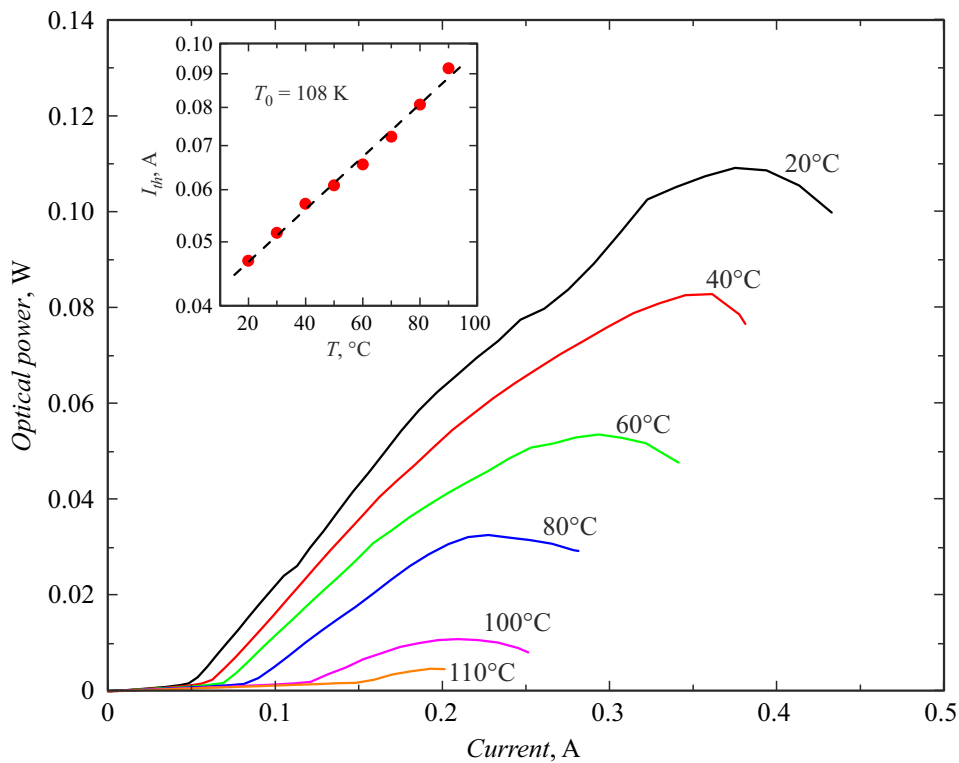


Figure 3. Light–current characteristics of a half-disk laser measured under continuous-wave pumping within the 20–110°C temperature range. The inset shows the temperature dependence of threshold current.

divergence of output radiation measured in the vertical and lateral directions was 65 and 15°, respectively. It should be noted that single-mode lasing has been observed in certain half-disk lasers within a specific current range in our earlier study [5]. We attribute this effect to a slight deviation of the position of the cleaved facet from the half-disk center.

The LCCs of half-disk lasers were measured within the 20–115°C temperature range under continuous-wave pumping. As the temperature increases, the threshold current of a half-disk laser rises, is differential efficiency decreases, and the maximum output power drops (Fig. 3). Lasing was observed up to a temperature of 113°C. Characteristic temperature T_0 within the range from 20 to 90°C was 108 K (see the inset in Fig. 3). The emission spectrum width increased insignificantly with the temperature.

Light–current characteristics of InGaAs/GaAs half-disk lasers with a half-ring contact were examined in a wide temperature range. The characteristics of the devices were enhanced considerably (relative to the results reported in our earlier studies) owing to an increase in the number of QWD layers in the active region and a reduction in the width of a half-ring metallic contact. At 20°C, an optical output power of 110 mW and a wall-plug efficiency of 18% were achieved; the maximum lasing temperature was 113°C. Further optimization of the design of microlasers may involve the introduction of even more QWD layers into the active region, miniaturization of devices, adjustment of the cleavage position with respect to the laser axis with the aim of controlling the lateral divergence and the mode composition, and alteration of the metallization geometry for the purpose of enhancing the efficiency of current injection and selection of the needed modes.

Funding

The authors acknowledge support from the Ministry of Science and Higher Education of the Russian Federation (project FSRM-2023-0010).

Conflict of interest

The authors declare that they have no conflict of interest.

References

- [1] N. Kryzhanovskaya, A. Zhukov, E. Moiseev, M. Maximov, *J. Appl. Phys.*, **54** (45), 453001 (2021). DOI: 10.1088/1361-6463/ac1887
- [2] A.M. Monakhov, V.V. Sherstnev, A.P. Astakhova, Y.P. Yakovlev, G. Boissier, R. Teissier, A.N. Baranov, *Appl. Phys. Lett.*, **94** (5), 051102 (2009). DOI: 10.1063/1.3075852
- [3] J.-D. Lin, L.-X. Zou, Y.-Z. Huang, Y.-D. Yang, Q.-F. Yao, X.-M. Lv, J.-L. Xiao, Y. Du, *Appl. Opt.*, **51** (17), 3930 (2012). DOI: 10.1364/AO.51.003930
- [4] F. Zubov, E. Moiseev, M. Maximov, A. Vorobyev, A. Mozharov, Yu. Shernyakov, N. Kalyuzhnyy, S. Mintairov, M. Kulagina, V. Dubrovskii, N. Kryzhanovskaya, A. Zhukov, *Photonics*, **10** (3), 290 (2023). DOI: 10.3390/photonics10030290
- [5] F.I. Zubov, E.I. Moiseev, M.V. Maximov, A.A. Vorobyev, A.M. Mozharov, Yu.M. Shernyakov, N.A. Kaluzhnyy, S.A. Mintairov, M.M. Kulagina, V.G. Dubrovskii, N.V. Kryzhanovskaya, A.E. Zhukov, *Laser Phys.*, **32** (12), 125802 (2022). DOI: 10.1088/1555-6611/ac996f
- [6] F.I. Zubov, E.I. Moiseev, M.V. Maximov, A.A. Vorobyev, A.M. Mozharov, N.A. Kaluzhnyy, S.A. Mintairov, M.M. Kulagina, N.V. Kryzhanovskaya, A.E. Zhukov, *IEEE Photon. Technol. Lett.*, **34** (24), 1349 (2022). DOI: 10.1109/LPT.2022.3216738
- [7] M.V. Maximov, A.M. Nadtochiy, S.A. Mintairov, N.A. Kalyuzhnyy, N.V. Kryzhanovskaya, E.I. Moiseev, N.Yu. Gordeev, Yu.M. Shernyakov, A.S. Payusov, F.I. Zubov, V.N. Nevedomskiy, S.S. Rouvimov, A.E. Zhukov, *Appl. Sci.*, **10** (3), 1038 (2020). DOI: 10.3390/app10031038

Translated by D.Safin